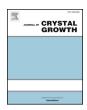
ELSEVIER

Contents lists available at ScienceDirect

## Journal of Crystal Growth

journal homepage: www.elsevier.com/locate/jcrysgro



## Investigation of defect creation in GaP/Si(001) epitaxial structures

Chaomin Zhang<sup>a,\*</sup>, Allison Boley<sup>b</sup>, Nikolai Faleev<sup>a</sup>, David J. Smith<sup>b</sup>, Christiana B. Honsberg<sup>a</sup>



- <sup>a</sup> School of Electrical, Computer and Energy Engineering, Arizona State University, Tempe, AZ 85287, USA
- <sup>b</sup> Department of Physics, Arizona State University, Tempe, AZ 85287, USA

#### ARTICLE INFO

Communicated by E. Calleja

Keywords:

A1. Crystal structure

A1. Defects

A1. High resolution X-ray diffraction

A3. Molecular beam epitaxy

B2. Semiconducting III-V materials

#### ABSTRACT

This work investigates defect formation and evolution associated with the deposition of GaP layers on precisely oriented Si(0 0 1) substrates. The GaP layers were grown with thicknesses ranging from  $\sim\!37$  nm to  $\sim\!2$  µm at a growth rate of 0.52 µm/hr using molecular beam epitaxy (MBE). The crystallinity of thin (37-nm) MBE-grown GaP layers was also compared with thin GaP layers grown by migration-enhanced epitaxy (MEE). The MBE growth procedure was shown to postpone relaxation of the epitaxial GaP layers up to a thickness of  $\sim\!250$  nm. Detailed analysis of high-resolution X-ray diffraction patterns and comparison with cross-sectional transmission electron micrographs clarified the defect formation mechanism. Thin GaP layers showed very low defect densities except for anti-phase boundaries, whereas substantial threading defects predominated in the thicker, noticeably relaxed structures.

#### 1. Introduction

It has been a longstanding goal of the semiconductor industry to integrate III-V alloys with Si substrates [1], in order to enable high performance microelectronic systems. For example, optoelectronic devices based on III-V/Si heterostructures can be realized by improving the crystal quality of pseudomorphic layers such as GaP. However, it is challenging to grow polar III-V materials using non-polar Si substrates. Defect creation and structural degradation during epitaxial growth of the III-V compounds due to the non-zero lattice mismatch, as well as the different crystal structure, are major obstacles that need to be addressed since the symmetry change at the diamond/zincblende (ZB) interface additionally impacts defect creation. Among many III-V alloys, only the GaPxN1-x ternary compound can be lattice-matched to Si substrates at the deposition temperature, but the direct growth of the nitride alloy is reported to generate crystalline defects via the creation of silicon nitride on the Si surface [2]. Gallium phosphide, which has a relatively small lattice mismatch (0.37%) with Si, is a strong candidate as a buffer layer for further III-V/Si integration, especially for multijunction solar cells [3], and other device applications [4,5]. The pseudomorphic growth of GaP-based materials on Si can help to mediate these problems by delaying the onset of defect creation. However, anti-phase domains (APDs), which are common for the epitaxial growth of polar material (GaP) on the non-polar material (Si) [6.7], are often associated with crystalline defects that are liable to act as deep-level traps in the forbidden gap of the device material. Furthermore, crystalline defects

created during heteroepitaxial growth, such as stacking faults and threading dislocations, are likely to decrease the minority-carrier lifetime of III-V solar cells and hence reduce their open-circuit voltage  $(V_{\rm oc})$ .

It has been shown that degradation of the crystal quality of GaP layers grown on Si substrates by molecular beam epitaxy (MBE) can be postponed by using the migration-enhanced epitaxy (MEE) technique and post-growth annealing [3,8-11]. Although epitaxial GaP layers grown on off-cut (≥4°) Si wafers have demonstrated reduced APD densities in the volume of the GaP layer [9,12-15], precisely oriented Si (001) wafers are required for many applications, such as complementary metal-oxide semiconductor (CMOS) devices for logic circuits [16], and are commonly used as the basis for solar cells. Thus, it is relevant to compare defect formation for GaP layers grown on off-cut and exactly oriented Si(0 0 1) substrates under nearly the same growth conditions. Depending on the amount of lattice mismatch and layer thickness, pseudomorphic layers can initially be grown almost coherently strained. However, beyond a specific layer thickness, which also depends on the growth conditions, the mismatch strain is accommodated by the creation of misfit dislocations [16]. In the GaP/Si heteroepitaxial system, which has small lattice-mismatch as well as a change in crystal symmetry, it becomes important to understand the thickness-related features of defect creation during stress relaxation and the compensation of polar/non-polar crystal asymmetry, and to compare with lattice-mismatched polar/polar, III-V on III-V, epitaxial structures [17]. The symmetry change, which will affect atomic

E-mail address: czhang86@asu.edu (C. Zhang).

<sup>\*</sup> Corresponding author.

incorporation during the initial stages of growth, will possibly lead to different features in defect creation during this thickness evolution.

In this work, we first demonstrate that thin ( $\sim\!50$  nm), almost defect-free GaP layers can grow by MEE on 4° off-cut Si substrates. The same growth conditions were then applied to a precisely oriented Si (0 0 1) substrate to reveal any different features in defect creation. Several thin GaP layers ( $\sim\!37$  nm) were then grown by conventional MBE procedures to establish the optimal V/III ratio. Finally, a set of GaP structures with different layer thicknesses up to 2  $\mu$ m was grown to elucidate the thickness-related defect formation process. High-resolution X-ray diffraction (XRD) and transmission electron microscopy (TEM) were used to establish correlations between growth conditions and the crystal quality of the epitaxial structures.

### 2. Experimental details

#### 2.1. Epitaxial growth of GaP-Si(001) structures

The GaP epitaxial layers were grown on  $Si(0\,0\,1)$  substrates using a solid-source Veeco GEN III MBE system with a P-valved cracker. The Si wafers consisted of n-type float-zone material, precisely oriented to  $(0\,0\,1)$  or  $4^\circ$  off-cut towards the  $[1\,1\,0]$  direction. This latter wafer misorientation is expected to assist in the formation of double atomic steps on the substrate surface and thereby minimize APD creation during GaP epitaxial growth [16].

Prior to deposition, the Si wafers were chemically cleaned using the standard RCA solution [18], which was finally combined with 5% hydrogen fluoride (HF) for surface refresh prior to loading in the MBE vacuum chamber. The GaP layers were grown on Si substrates that had been preheated at 820 °C (thermocouple reading and hereafter) for 5 min to fully remove residual silicon native oxide and restore the double-domain  $(2\times1)/(1\times2)$  reconstructed surface structure. Surface reconstructions during preheating and deposition were monitored *in situ* by reflection-high-energy electron diffraction (RHEED). After annealing, the substrate temperature was decreased to the deposition temperature selected for epitaxial growth, as described below.

Two MEE-grown GaP-Si(001) heterostructures of 50-nm GaP layer thickness were deposited at substrate temperatures of 440 °C onto off-cut (MEE-I structure) and precisely oriented (MEE-II structure) Si wafers using the same Ga and P fluxes. The deposition loop, which consisted of a sequence of 5-second Ga deposition, 1-s pause with closed Ga and P sources, 8-s exposure under P flux, and 5-s pause, was repeated for a total 184 cycles. Before commencing MEE growth, the P shutter was opened for 30 s and then closed for 12 s before the initial Ga deposition. The approximate P to Ga flux ratio was set at  $\sim$  5:1. All flux ratios used in this work were the beam equivalent pressure ratios measured by beam flux monitor (BFM).

In addition to the MEE growth, conventional MBE growth of the GaP layers was investigated. To determine the optimum conditions for GaP deposition on precisely oriented Si(001) substrates, growths were conducted at a substrate temperature of 580 °C, using different V/III (P/ Ga) ratios ranging from 6.9 to 3.1 and a growth rate of  $\sim 0.52 \,\mu\text{m/hr}$ . Several GaP layers were epitaxially grown with thicknesses of 37 nm, which is well below the GaP/Si critical thickness. At the initiation of growth, the P shutter was open for 20 s for P deposition, then 10 periodic loops of (GaP-P) short-period deposition with 5-s GaP deposition and 5-s pause under P-flux, were applied to improve the planarity of the growth front [19]. The main growth sequence was then commenced. The final set of GaP-Si(001) epitaxial structures with GaP layer thicknesses ranging from 37 nm up to 2 µm were grown by MBE using a P/Ga ratio of ~4.5, which had been identified by XRD and AFM as optimal for GaP epitaxial growth at 580 °C on the precisely oriented wafers.

#### 2.2. Characterization methods

High-resolution XRD studies were performed using an X'Pert MRD diffractometer with a multilayer focusing mirror under double- and triple-axis alignment. Hybrid 4-bounded Ge(2 2 0) monochromator ensured collimated and almost monochromatic Cu K $\alpha$ -1 incident radiation with 18 arc.sec divergence angle, while a 3-bounded Ge(2 2 0) analyzer (12 arc.sec acceptance angle) provided spatially separate coherent and diffuse-scattered radiation in the vicinity of diffraction spots for detailed analysis of crystal quality. Coherent double-crystal (DC) and triple-crystal (TC)  $\omega$ -20 and  $\omega$  rocking curves (RCs), and TC Reciprocal Space Maps (RSMs) in the vicinity of (0 0 4) and (2 2 4) reflection spots were used to determine layer composition and to analyze strain conditions, and also to specify the type, spatial distribution, and density of crystal defects. Atomic force microscopy (AFM) was conducted by multimode scanning probe microscope (SPM) to study the surface morphology.

Specimens suitable for TEM observation were prepared using focused-ion-beam milling with a dual-beam FEI Nova-200, as well as additional argon-ion-milling to further reduce the sample thickness and to remove any surface-milling artifacts. Observations were made with a Philips-FEI CM200 high-resolution electron microscope, operated at 200 keV, and a probe-corrected ARM-200F scanning transmission electron microscope, also operated at 200 keV. Cross-section observations were made along  $\{1\ 1\ 0\}$ -type zone axes so that the surface normal would be perpendicular to the incident-beam direction.

#### 3. Results

#### 3.1. Structural investigation of MEE-grown structures

The two 50-nm-thick MEE-grown GaP layers (MEE-I and MEE-II structures) were observed using XRD. The high crystal quality of the GaP epitaxial structure grown on the off-cut Si wafer is confirmed by a clear interference pattern that extended widely around the GaP peak in the DC  $\omega$ -20 RC (Fig. 1a, black curve), and just the narrow coherent central peak in the GaP(004) TC  $\omega$  RC (Fig. 1b, black curve). The extended interference pattern obtained for the DC  $\omega$ -20 RC reveals the high vertical coherence of the epitaxial layer, close to the real layer thickness. In general, this means that the density of crystal defects in the volume of such layers, roughly estimated by the Full-Width-Half-Maximum of the central substrate peak (FWHM  $\approx$  9.6 arc.sec) as less than  $\sim 10^5$  cm<sup>-2</sup>, is insufficient for overlap of elastic strain, induced by the closest defects, which would bend the structure and deteriorate crystal quality, and diminish the spatial coherence of the layer. The almost zero diffuse background on the tails of the  $\boldsymbol{\omega}$  RC confirms that additional elastic stress and bending of the structure (approximate radius is > 100 m), induced by crystal defects, are really very low [20].

In comparison with the offcut structure, the DC  $\omega$ -2 $\theta$  RC of the MEE-II structure (Fig. 1a, red curve<sup>1</sup>) demonstrates substantial diffusion of the interference pattern around the GaP layer peak due to layer bending and hence deterioration of X-ray vertical coherence in the GaP layer. This would most likely be caused by elastic stress induced by the core of dislocations created during epitaxial growth. Among them, {1 1 1} spatially distributed stacking faults, which intersect in the volume of the layer, could lead to the creation of edge segments [21].

Simultaneous reduction of intensity and increase of the FWHM of the coherent central layer peak ( $\sim\!14.3$  arc.sec) of the MEE-II TC  $\omega$  RC (Fig. 1b, red curve), as well as the appearance of the wide diffuse base superimposed on the coherent peak, clearly mark the onset of defect creation. The FWHM of the diffuse base ( $\approx\!600$  arc.sec) roughly estimates the density of created defects ( $\sim\!1.3\times10^9\,\mathrm{cm}^{-2}$ ), while the low

<sup>&</sup>lt;sup>1</sup> For interpretation of color in Figs. 1 and-6, the reader is referred to the web version of this article.

## Download English Version:

# https://daneshyari.com/en/article/11026326

Download Persian Version:

https://daneshyari.com/article/11026326

<u>Daneshyari.com</u>